COBEM 2021 26th International Congress of Mechanical Engineering
November 22-26, 2021, Virtual Congress, Brazil
ABCM Associação Brasileira de Engenharia e Ciências Mecânicas

COB-2021-1464
EXPERIMENTAL MEASURING PROCEDURE FOR WEAR AND COEFFICIENT OF FRICTION OF POLYMERIC CONVEYOR IDLERS

Daniel Estefano Pacholok
Fernanda Kouketsu
Diego Aguiar Martins
Tiago Cousseau
Carlos Henrique da Silva
Universidade Tecnológica Federal do Paraná, Av. Sete de Setembro, 3165, 80230901, Curitiba, Brasil
danielpacholok@hotmail.com
fe.kouketsu@gmail.com
diegoaguiar@alunos.utfpr.edu.br
tcousseau@utfpr.edu.br
carloshs@utfpr.edu.br

Abstract. *The rubber wheel abrasion test, standardized by ASMT G-65, is an experimental procedure widely used to assess the abrasive wear resistance of materials. This work presents a study of different experimental procedures for polymeric roller abrasion tests with different sample geometries. Tests were carried out with segments of commercial idler rolls, nominated as ring samples. The ring samples were evaluated in two conditions: rotating and non-rotating. The rotating condition simulates the usual field operating conditions, while the non-rotating condition simulates the situation in which the idler roll is locked due to bearing failure. The tests with High Density Polyethylene (HDPE) and Ultra-High Molecular Weight Polyethylene non-rotating ring samples were performed with a normal force of 200 N during 10 minutes (1,420 meters); and the tests with rotating ring samples were performed with 250 N and 40 hours (3.4 E+6 meters). In all tests, ANB 100 sand was used. Worn surfaces were evaluated and compared to idlers that operated for 1 year in the field using SEM and contact profilometry. The wear values and wear mechanisms of the field and lab-tests idler roll materials point towards an improved method to evaluate idlers wear resistance.*

Keywords: *polymeric abrasion, dry-sand rubber-wheel, ASTM G65, ring samples.*

1. INTRODUCTION

In modern truckless ore transportation system, conveyor belts play a mayor role due to inherent advantages as safety operation, economy, reliabilyty and high range of loading capacity (CEMA, 2007). This system consists of long rubber belts suported by steel rollers. When one roller stops rotating due to failure of its rolling bearing, which is the main failure mechanism of stell idlers, a combined action of the friction between conveyor belt and idler roll with abrasion caused by external particles may wear off the idler steel roll leaving some sharp edges exposed. This in turn may cut the belt and lead to a catastrophic failure (Fiset and Dussault, 1993). The transportation system maintenance, in particular idlers replacement, is quite difficult due to the heavy weight of steel idlers and the limited access. In order to minimize the risks of belt cutting and to improve maitenance conditions, polymeric idler rolls have been proposed as an alternative to steel idler rolls. Worn polymeric idlers sharp edges do not cut the conveyor belt and their low weight facilitates maintenance, increasing the overall system reliability. Even though polymeric idlers present clear advantages over stell idlers, their durability is still unknow. Polymeric materials used to present lower abrasion resistance than steel, therefore, polymeric idlers mechanical resistance might get compromised by its diameter reduction due to abrasion wear. Based on that, it is of utmost relevance to develop a methodology to evaluate the abrasion resistance of polymeric idlers.

The dry-sand rubber wheel test is commonly used to evaluate the abrasion resistance of materials under three-body abrasive conditions. The main usage of this test is to rank materials that will undergo low stress abrasion such as agricultural tools, hoppers and conveyor belts idlers (Stevenson and Hutchings, 1996). The aparatus is comprised of a plane specimen which is loaded against a rotating rubber wheel while sand is fed into their interface, abrading the specimen. The standard apparatus is shown in Fig. 1. Though the standartized dry-sand rubber wheel test closely simulates the conditions of a blocked idler roll, when the rotational speed has halt, to study the behavior of idler rolls operating under normal conditions, a modified apparatus of the ASTM-G65-16 dry-sand rubber wheel was designed and built. The design was inspired in the one used by Fiset and Dussault, where the mounting allows rotating spicemens.

Therefore, the present paper presents a methodology to access idler rolls abrasion resistance in conditions similar to the ones observed in the field in order to select materials that are relevant for this applicaiton.

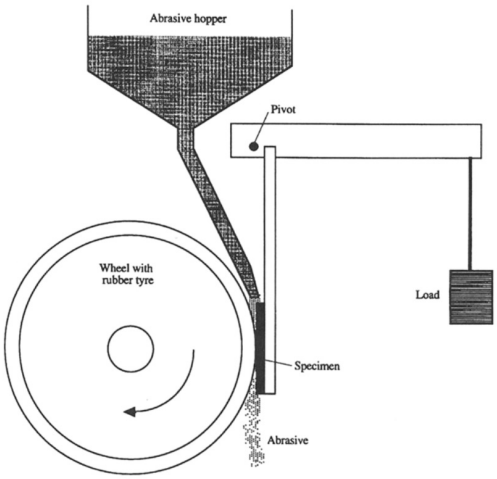

Figure 1. ASTM G65 dry-sand rubber wheel apparatus.

2. EXPERIMENTAL METHOD AND MATERIALS

The device used to fix ring samples is composed by a cone-disc mounting apparatus. The ring spicemen consists of a section of commercial idlers, more accurately simulating field conditions. The mounting apparatus is shown in Fig. 2 and in Fig. 3.

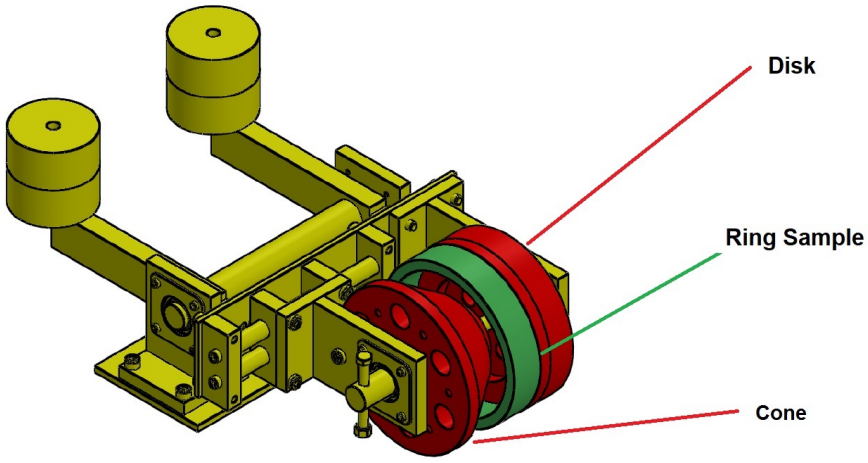

Figure 2. Ring sample rubber wheel apparatus.

Figure 2 shows the cone-disc mounting apparatus in red color. This aparatus makes possible to mount sections of commercial idlers of diferent diameters easily.

Also, the developed tester is assembled with a pivot and counts with load cells to measure normal and frictional forces. Due to the size of the cone, it was needed to balance the system by applying some dead weight to release the load in the frictional force cell. The normal force is aplied by a pneumatic actuator which is driven by a PID system. The abrasometer runs driven by a PLC controller in which can be setted the rubber wheel rotation speed, the applied normal force and the duration time of the tests. The PLC has a data acquisition of 2.5 points/second, meaning the PLC reads the load cells 2.5 times per second and transfers the data to the computer once at a minute. Figure 3 shows the abrasometer during a non-rotating condition testing. It can be seen the frictional force load cell positioned bellow the cone-disk device. Also can be noticed the activated blocking screw halting the rotation of the spicemen fixing divice.

The sand is stored in a reservoir above the equipment and is delivered into contact zone through a hosepipe that ends in a nozzle designed according to ASTM G65 standard. The sand flow obtained using this system feeded with ABN 100 brazillian sand is 220 g/min. The ABN 100 brazillian sand has an average particle size of 226,10 μm. The sand curtain, as can be seen in Fig. 3 is properly stream-lined and narrow.

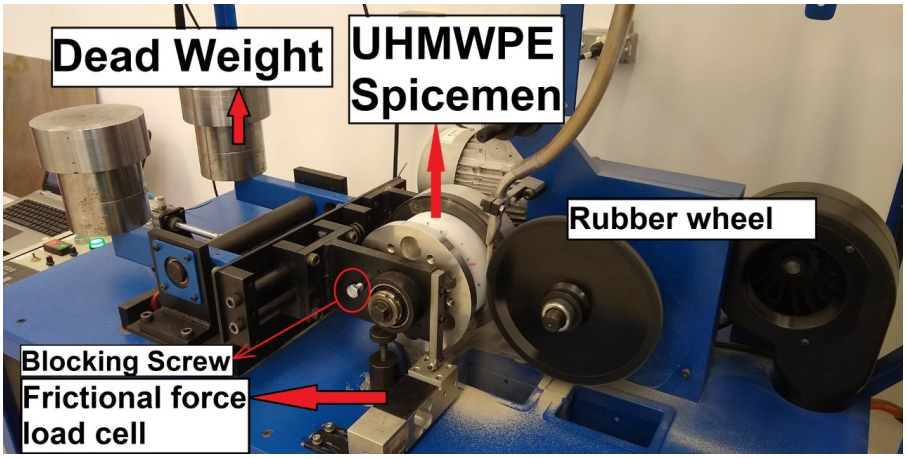

Figure 3. Working abrasometer at a non-rotating condition testing.

The tests were carried out in two conditions: rotating and non-rotating. The blocking screw intends to block the rolling freedom of the sample, allowing the non-rotating tests to be carried out. As shown in Fig. 2 the spicemen used have ring geometry. Thus, the rotating conditions is the one where the device allows the spicemen to rotate when in contact with the rubber wheel; and in the non-rotating condition the blocking screw is activated, halting the rotation of the spicemen fixing device.

The parameters for each condition are described in Tab. 1.

Table 1. Experimental parameters.

Parameter	Rotating	Non-rotating
Rotation speed [rpm]	200	200
Normal Load [N]	250	200
Abrasive particles	ABN100 Sand	ABN100 Sand
Abrasive flow [g/min]	220	220
Duration Time [min]	2400	10
Sliding distance [number of revolutions]	480 E+3	2000
Sliding distance [m]	342 E+3	1436

As shown in Tab. 1, the normal load in the rotating condition is greater. This decision was made aiming to increase wear of spicemen reducing the testing time needed to be possible measuring wear with gravimetry method. Thus, the load and testing time of the non-rotating tests were smaller than the rotating tests in order to reduce wear; otherwise the wear scars would get too large.

2.1 Materials

The test in non-rotating condition were performed three times for each material specimen. But, due to long duration time of the rotating tests, in this condition the tests were taken once with each material.

The polymer samples tested were taken from commercial rollers made of HDPE filled with carbon black (3.6% weight) and UHMWPE. Table 2 shows the dimensions of the samples. Though taken from commercial rollers, the spicemen were machined to reduce radial runout. Table 3 shows some mechanical properties of the tested polymers.

Table 2. Dimensional characteristics of the used polymer spicemen.

Material	Diameter [mm]	Width [mm]	Thickness [mm]
HDPE+ 3.6%CB	160	31.6	21.5
UHMWPE	160	18.0	14.5

It can be seen that, beeing both polyethilenes, the polymer presents similar mechanical properties, such as density, and Shore D Hardness. Though, it is shown in this paper the rubber wheel abrasion tests do rank the abrasive wear resistance of these polymers spicemen with acceptable reliability.

The spicemen were subjected to gravimetry in an analytical balance Marte - AUX320 before and after each test, and

Table 3. Some mechanical properties of the tested polymers.

Material	Density [g/cm^3]	Shore D Hardness	Yield Strength [MPa]	Elongation at Yielding [%]
HDPE+ 3.6%CB	0.965	62	26	11
UHMWPE	0.9316	60	21.8	32.6

then the mass difference converted to volume loss using Eq. 1, according to ASTM-G65-16 standard.

$$V = 1000(\frac{m}{p}) \tag{1}$$

where $[V]$ is the wear volume in [mm^3]; $[m]$ is the mass difference after testing in [g]; and ρ is the material density in [g/mm^3].

Moreover, since the ASTM-G65-16 standard demands the wear to be evaluated using an rubber wheel with diameter of 228.60 mm (9") to a minimum diameter of 215.90 mm (8.1/2"); it is required to update the diameter to properly evaluated wear using the Eq. 2.

$$V_{adj} = V\frac{228,60}{D_{adj}} \tag{2}$$

Where $[V_{adj}]$ is the corrected value of wear; $[V]$ is the wear obtained in Eq. 1; and $[D_{adj}]$ is the adjusted diameter at the end of testing.

Furthermore, after the testings and the gravimetric measurements, the spicemen were cut and subjected to scanning eletron microscope (SEM) to assess the topography of the worn surfaces. Also, once the adapted abrasion tester counts with a load cell to measure the frictional force, it was possible to compute the coefficient of friction presented during the tests.

3. EXPERIMENTAL RESULTS AND DISCUSSION

The results for wear volume loss and coefficient of friction (COF) of the tests carried out in non-rotating condition are shown in Fig. 4.

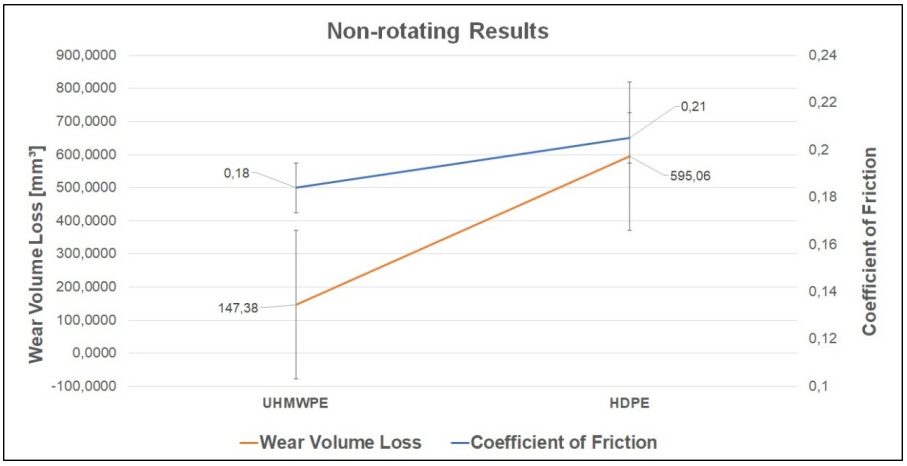

Figure 4. Results for wear volume loss and coefficient of friction of non-rotating tests.

It can be seen that the UHMWPE spicemen had an average volume loss due to wear about 75% smaller than the HDPE+3,6%CB spicemen. Also, the coefficient of friction values were close, but still the UHMWPE spicemen presented an average COF of 0.18 while the HDPE+3,6%CB presented 0.20 average COF.

As mentioned, the COF of testings were computed by the ratio between the measured normal and tangential forces. The last 300 seconds of data were taken as steady state and used to calculate the COF for the tests. The Fig. 5 shows a comparison of the curves of friction for typical non-rotating tests with each spicemen.

Bhushan postulates that friction and wear are affected by changes in the conditions of mating surfaces. Thus, in a tribologycal system comprised of a rubber wheel and a polymer with sand particles as interfacial elements, the polymer itself can suffer surface changes; as the wear scar grows larger the sand can settle a preferencial path and change movement pattern through the contact zone. This change in movement pattern may affect the wear mechanisms, as previously related by Fang *et al.* (1993). Also, grooves can be made in the rubber wheel surface. All these phenomena contributes to an

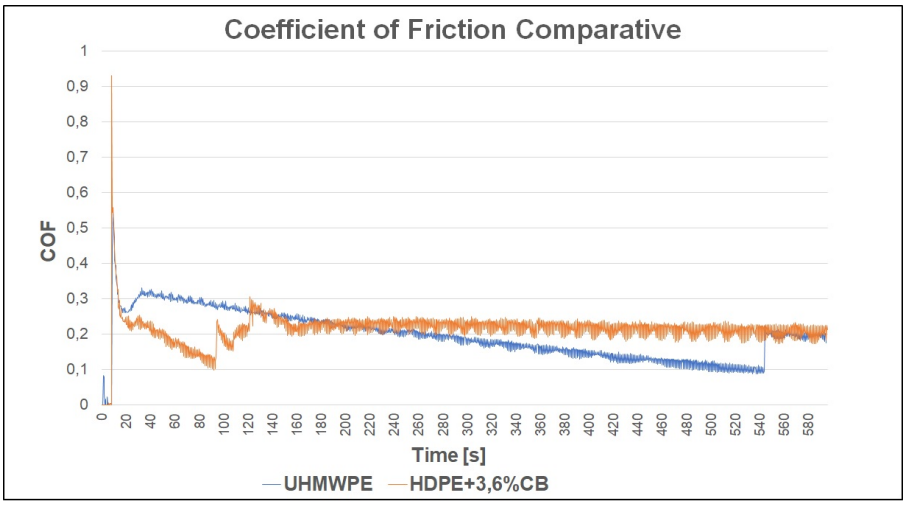

Figure 5. Coefficient of Friction curves for a typical test of each material spicemen.

unstable friction force to be observed. A run in period can be observed in Fig. 5, which is expected and, as can be seem, HDPE presents a run in period of 160 s. Although, UHMWPE doesn't clearly present an steady-state COF, but at time-to-time it suffers a sudden raise and then starts to decrease again. Stachowiak and Andrew mentioned a similar behavior for this material, presuming it was a sinergic effect of wear and material fusion at surface. The authors explains this phenomenon occurs due the sum of small fused portions of material at the surface; which are removed and then the surface is renewed.

Similar results for wear abrasion have been previously reported by Budinski, a work which presented UHMWPE material showing higher abrasion resistance and lower coefficient of friction than HDPE.

Nonetheless it is interesting to notice the results for the tests in rotating condition, which are presented in Fig. 6.

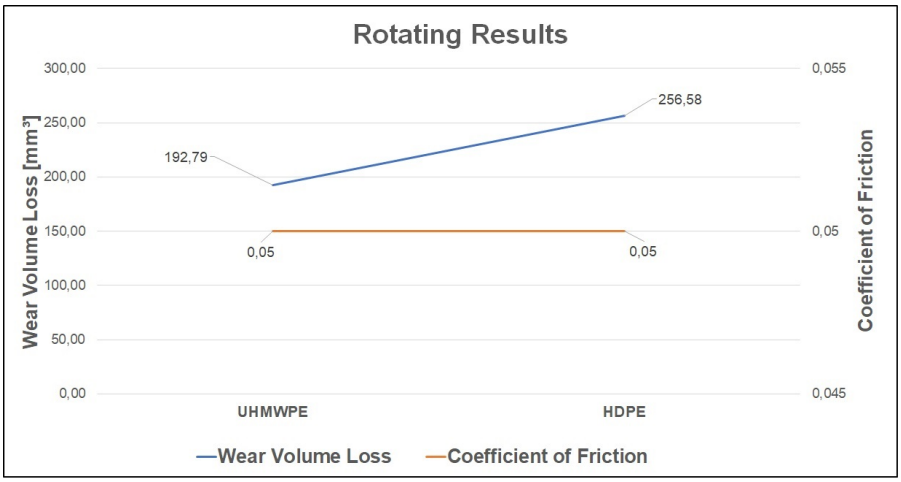

Figure 6. Wear volume loss results for rotating condition tests.

One can notice that UHMWPE specimen remains presenting lower wear volume loss even under three body abrasion test (rolling conditions). However the ratio of wear has changed from 75% to only 25% between the materials.

The average values of wear volume loss and friction are presented in Tab. 4.

Table 4. Experimental results for wear volume loss and coefficient of friction.

Condition	**Material**	**Volume loss [mm^3]**	COF
Rotating	UHMWPE	192.79	0.05
Rotating	HDPE+3.6%CB	256.58	0.05
Non-Rotating	UHMWPE	147.38 ± 52.43	0.18 ± 0.04
Non-Rotating	HDPE+3.6%CB	595.06 ± 66.44	0.20 ± 0.02

It can be also noticed that wear volume loss of the UHMWPE spicemen were 23% greater for the rotating condition

than for the non-rotating condition. This result can be related to the predominant wear mechanism in each test condition. Fang *et al.* reports that micro-cutting takes place in case forces that are not present in rotation of particles condition occurs. Thus, once the two mating bodies present the same tangencial speed, there are no tangencial forces acting in the sand particles, resulting that the indentation wear mechanisms to be predominant in this condition.

The phenomena towards contact zone during non-rotating tests are complex. From beginning to the end of the test the contact between rubber wheel and the spicemen changes from non-conformal to a conformal contact. Also, the contact area increases during the test, reducing the contact pressure. These changes are not so clearly seem in the rotating tests.

The SEM images presented in Fig. 7 (a) and (b) shows the surfaces of HDPE+3.6%CB worn in non-rotating test and rotating test. Figure 7 (c) shows the surface of an idler which has been operating in field for one year.

The image of the non-rotating worn surface was taken from the center of wear scar and the rotating worn surface image was taken from the midle width of the wear scar. The red arrows points the sliding direction of the rubber wheel and the rotating direction of the idler roller.

Furthermore, the SEM images presented in Fig. 7 shows that for the spicemen tested in rotating conditions the wear scars were origined from particle indentation due the rolling of particles along the polymer surface. The rotating condition worn surface was quite similar to that surface observed in idler roller.

Figure 7. SEM micrography of worn spicemen and from a worn surface of an field operating idler.

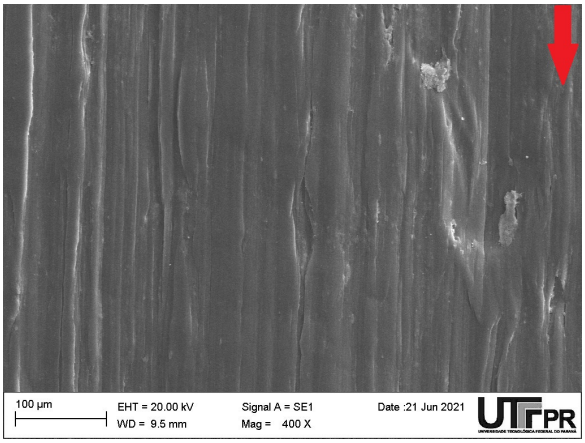

(a) HDPE Non-rotating.

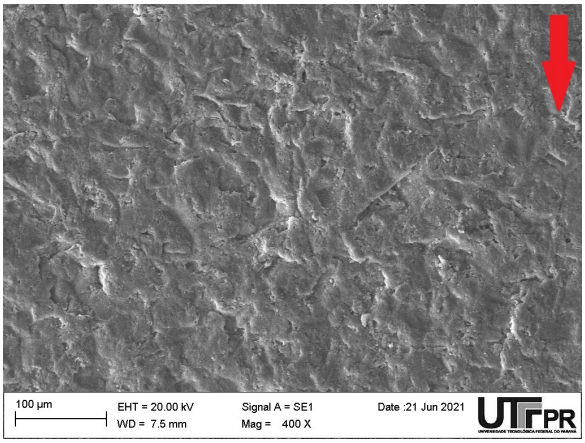

(b) HDPE Rotating.

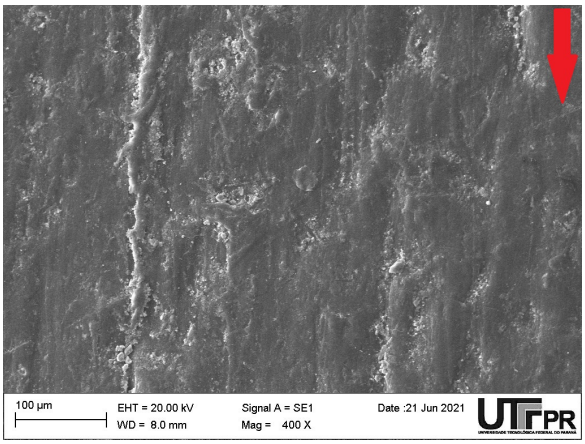

(c) In Field Operating Idler.

Czichos and Winer mentions the importance of systems structure and its elements, properties and interrelations. Part of the tribologycal systems structure is the interfacial element and how it interacts with the two mating surfaces. Fang *et al.* relates the relation of particle pattern movement with wear mechanisms and its effect in wear volume loss observed. The author discuss the wear may be caused by cutting mechanisms, probably being promoted by sliding particles; and by deformation mechanisms, being attributed to rolling particles. Also, higher wear volume lossess are pointed as result of grooving and scratching while pitting may results in mild wear volume lossess. Althogh Nahvi *et al.* studies steel abrasion, the authors also mention higher wear caused by sliding of particles; discussing the increased attack angle of engasted particles, promoting cutting as efficient mode of material removal.

The rotating worn surface topography sugests rolling motion of particles and indentation with little directionality, which leads to plastic deformation wear mode; otherwise, the non-rotating worn surfaces sugests sliding of particles,

leading to microscratching and microcutting wear mechanisms.

The surface aspect of the worn idler roller sugests both indentation and scratching with clear directionality.

There are many parameters that may change the movement particle pattern and so the wear mechanisms. Some of these parameters such as the normal load and the substract material hardness of metals were studied by Fang *et al.* and by Nahvi *et al.*. In this work, its sugested the main cause is the motion between rubber wheel and the spicemen. Thus, the wear mechanisms presented in rotating worn surface was found to be quite similar to that observed in idler rollers.

4. CONCLUSIONS

From the results obtained, it can be concluded that the equipment allows to rank polymers with quite similar mechanical properties using both the rotating and non-rotating types of tests, being suitable to assess the abrasion of materials by different wear mechanisms.

Even further, it could be saw the wear mechanisms comprehending the two types of tests, being the cutting wear predomintly observed in non-rotating tests and plastic deformation by particle rolling predominantly seen in rotating tests. Also, it could be concluded the wear mechanisms present in rotating tests are similar to the ones observed *in situ* conditions.

5. ACKNOWLEDGEMENTS

The authors are grateful to VALE for financial suport of the project 23064.023748/2018-79; to the Mechanical and Materials Engineering Post-Graduation Program of UTFPR - CT; and to Multi-User Center for Materials Characterization - CMCM of UTFPR-CT.

6. REFERENCES

ASTM-G65-16, S., 2017. *American Standard for Testing Materials. Measuring abrasion using the dry sand/rubber wheel apparatus, Annual Book of Standards*. ASTM.

Bhushan, B., 2000. *Modern tribology handbook, two volume set*. CRC press.

Budinski, K.G., 1997. "Resistance to particle abrasion of selected plastics". *Wear*, Vol. 203, pp. 302–309.

CEMA, 2007. *Belt Conveyors for Bulk Materials*. Conveyor Equipment Manufacturers Association, USA, 2nd edition.

Czichos, H. and Winer, W., 1978. "Tribology: a systems approach to the science and technology of friction, lubrication and wear (tribology series, 1)".

Fang, L., Kong, X.L., Su, J.Y. and Zhou, Q.D., 1993. "Movement patterns of abrasive particles in three-body abrasion". *Wear*, Vol. 162-164, pp. 782–789.

Fiset, M. and Dussault, D., 1993. "Laboratory simulation of the wear process of belt conveyor rollers." *Wear*, Vol. 162-164, pp. 1012–1015.

Nahvi, S.M., Shipway, P.H. and McCartney, D.G., 2009. "Particle motion and modes of wear in the dry sand–rubber wheel abrasion test." *Wear*, Vol. 267, pp. 2083–2091. URL `http://doi:10.1016/j.wear.2009.08.013`.

Stachowiak, G. and Andrew, B., 2005. *Engineering Tribology, Third Edit*. Elsevier, 832p.

Stevenson, A.N.J. and Hutchings, I.M., 1996. "Development of the dry sand/rubber wheel abrasion test." *Wear*, Vol. 195, pp. 232–240.

7. RESPONSIBILITY NOTICE

The authors are solely responsible for the printed material included in this paper.